ACS OMEGA

Open Access

http://pubs.acs.org/journal/acsodf

Article

Optimizing Lead-free $MASnBr_3$ Perovskite Solar Cells for High-Efficiency and Long-Term Stability Using Graphene and Advanced Interface Layers

Muhammad Haneef, Sofia Tahir,* Haitham A. Mahmoud, Adnan Ali, and Arslan Ashfaq*

Cite This: *ACS Omega* 2024, 9, 7053−7060

Read Online

ACCESS | Metrics & More | Article Recommendations

ABSTRACT: Perovskite solar cells (PSCs) have garnered significant attention in the scientific community due to their rapid increase in performance. Inorganic perovskite devices have been noted for their high performance and long-term stability. This study introduces a device optimization process guided by modeling to produce high-efficiency PSCs using lead-free n−i−p methylammonium tin bromide ($MASnBr_3$) materials. We have thoroughly examined the impact of both the absorber and interface layers on the optimized structure. Our approach utilized graphene as the interface layer between the hole transport and absorber layers. We employed zinc oxide (ZnO)/Al and 3C−SiC as interface layers between the absorber and electron transport layers. The optimization process involved adjusting the thicknesses of the absorber layer and interface layers and minimizing defect densities. Our proposed optimized device structure, ZnO/3C−SiC/$MASnBr_3$/graphene/CuO/Au, demonstrates theoretical power conversion efficiencies of 31.97%, fill factors of 89.38%, a current density of 32.54 mA/cm^2, a voltage of 1.112 V, and a quantum efficiency of 94%. This research underscores the ability of $MASnBr_3$ as a nontoxic perovskite material for sustainable energy from renewable sources' applications.

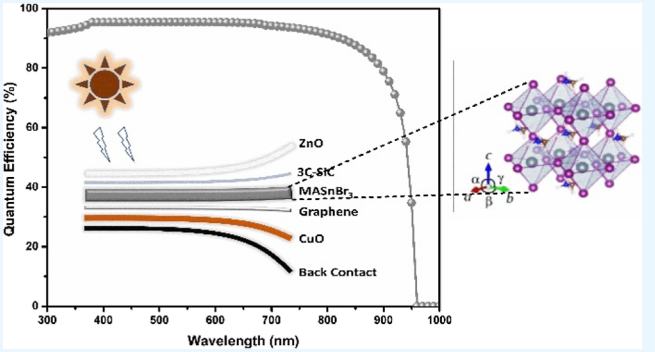

1. INTRODUCTION

The growing drive toward a clean and renewable energy future has sparked heightened enthusiasm for sustainable energy sources with a particular focus on photovoltaic (PV) technologies. Perovskite solar cells (PSCs) have emerged as a promising substitute for conventional silicon (Si)-based devices, primarily due to their exceptional performance, cost effectiveness, and possible scalability.[1] PSCs' remarkable PV capabilities can be attributed to their outstanding optoelectronic characteristics, fine-tuned alignment of a finely tuned energy band, and refined interface characteristics.[2] Nonetheless, the enduring durability of perovskite devices remains a point of contention as they experience degradation faster than conventional cells, necessitating more frequent replacement. The effectiveness of PSCs is intricately tied to the stability and efficiency of the solar cell's charge transportation and light absorption mechanisms. Specifically, the interface between the absorber layer, the hole transport layer (HTL), and the electron transport layer (ETL) on the hole and electron selective side of PSCs play a pivotal role.[3,4] To function effectively as a hole transport material (HTM), several criteria must be met: its valence band maximum should surpass that of the absorber layer, it must exhibit a high hole movement to extract hole charge from the absorber layer efficiently, and it should yield an unchanging and dense film during the processing phase.[5] The composition and properties of these layers substantially impact the cell stability and efficiency. The highest performance is achieved when zinc oxide (ZnO) is employed as the ETL in PSCs.[6] The maximum performance of the PSCs is achieved when CuO is used as the HTM.[7] Numerical simulations showed efficiencies of 24.17, 25.36, and 24.50% when zinc oxide was employed as the ETM layer with Spiro-MeOTAD, CuO_2, and PEDOT:PSS, as the HTM, respectively, with $MASnI_3$ absorber layer.[8] Graphene was used as an interface layer due to its high electrical properties, wide absorption spectrum, high charge carrier mobility, and increased stability of the PSC structure.[9] The ZnO/Al material was synthesized with the best optical properties, high charge carrier concentration and mobility with a high absorption model.[10] The 3C−SiC material was used as a buffer layer and increased the recombination rate and stability of the structure.[11] Simulations of a PSC-based $MASnI_3$ material layer, using

Received: November 11, 2023
Revised: January 12, 2024
Accepted: January 22, 2024
Published: January 31, 2024

https://doi.org/10.1021/acsomega.3c08981
ACS Omega 2024, 9, 7053−7060

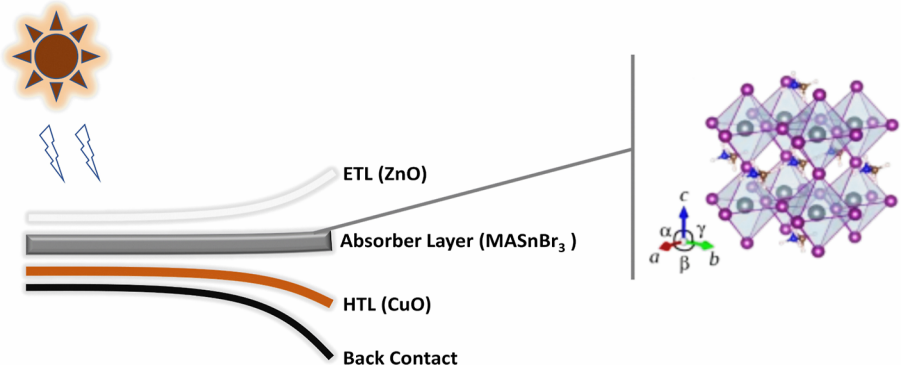

Figure 1. Schematic diagram of the initial cell structure with the absorber layer structure.

titanium dioxide as the ETL layer and CuSCN as the HTL layer, resulted in a peak PCE of 28.32%.[12] Mushtaq et al. reported the highest performance of $MASnBr_3$-based PSCs with optimization of different ETL, HTL, and defect densities.[13] The interface layers between the different layers play a vital role in the performance.

In this work, we have numerically simulated a $MASnBr_3$-based device with CuO as the HTM and ZnO as the ETM in the structure. We have optimized the device's efficiency by adding the graphene interface layers between the HTL and absorber layer and ZnO/Al and 3C−SiC interface layers between the perovskite layer and ETL and changing their densities and thicknesses. We have investigated the maximum performance with a suitable interface layer with appropriate thickness and defect density.

2. DEVICE STRUCTURE

Theoretical investigations hold valuable insights for experimental work, as simulations provide a more in-depth exploration of intrinsic factors and underlying physical principles in real-world applications, thus conserving both time and resources for the scientific community.[14] In this research, we have conducted numerical simulations of perovskite cells using the SCAPS-1D software.[15] The performance of solar cells is achieved by solving the three equations, including the Poisson equation, the continuity equation for electrons, and the continuity equation for the hole.[16]

$$\text{Poisson equation: } -\frac{\partial}{\partial x}\left(-\varepsilon(x)\frac{\partial V}{\partial x}\right) = q[p(x) - n(x) + N_D^+(x) - N_A^-(x) + p_t(x) - n_t(x)] \quad \text{(i)}$$

$$\text{Continuity equation for the hole: } \frac{\partial p}{\partial t} = \frac{1}{q}\frac{\partial J_p}{\partial x} + G_p - R_p \quad \text{(ii)}$$

$$\text{Continuity equation for electron: } \frac{\partial n}{\partial t} = \frac{1}{q}\frac{\partial J_n}{\partial x} + G_n - R_n \quad \text{(iii)}$$

where q is the charge, ε is the dielectric permittivity, V is the potential, $p(x)$ is the free-hole concentration, $n(x)$ is the free-electron concentration, $N_D^+(x)$ is the ionized donor concentration, $N_A^+(x)$ is the ionized acceptor concentration, $p_t(x)$ is the hole trap density, J_n is the current density of the electron, J_p is the current density of the hole, G_n is the electron-generation rate, G_p is the hole-generation rate, R_n is the recombination rate of an electron, and R_p is the recombination rate of the hole.

This approach allows us to derive the PSCs' spectral response and current−voltage (I−V) properties. The configuration of the $MASnBr_3$-based devices used in our study is depicted in Figure 1.

The $MASnBr_3$ material is the perovskite layer packed between the ETM (ZnO) and HTM (CuO). The input device parameters were taken from published work, as depicted in Table 1. The device operates at a fixed temperature of 300 K. All numerical calculations are conducted under an incident light intensity of 1000 W/m^2, corresponding to the air mass of 1.5 G solar band. In practical PSCs, the interface often exhibits a range of intricate defects, including lattice mismatches and interfacial dislocations.[17] In real experiments, these defects could result in the loss of charge transporters near the interface, lowering the operational amount of charge in the device and the cell's V_{oc}. The initial calculated parameters were PCE = 27.02%, FF = 81.19%, J_{sc} = 32.59 mA/cm^2, and V_{oc} = 1.02 V.

Table 1. Initial Input Parameters of the Cell Structure

properties	CuO	$MASnBr_3$	ZnO
thickness (nm)	100	500	50
band gap (eV)	2.170	1.300	3.300
electron affinity (eV)	3.200	4.170	4.1
valence band density of state (1/cm^3)	2.500×10^{20}	2.200×10^{18}	1.000×10^{19}
conduction band density of state (1/cm^3)	2.50×10^{20}	1.80×10^{18}	1.00×10^{18}
mobility of electron μ_e [cm^2/(V s)]	8.00×10^{1}	1.60×10^{0}	9.00×10^{0}
mobility of hole μ_p [cm^2/(V s)]	8.00×10^{1}	1.60×10^{0}	1.00×10^{2}
donor charge density N_D (1/cm^3)	0	1.00×10^{13}	1.00×10^{18}
acceptor charge density N_A (1/cm^3)	1.00×10^{18}	1.00×10^{13}	1.00×10^{5}
defect density N_T (1/cm^3)	1.00×10^{15}	1.00×10^{14}	2.00×10^{17}
references	13	13	13

3. RESULTS AND DISCUSSION

3.1. Optimization of the Interface Layer. In PSCs, interface layers are critical, because they greatly impact stability and performance. In this study, we have used the different interface layers, such as graphene is used in the HTL and absorber layer and ZnO/Al and 3C−SiC are used in the ETM and absorber layer. The input parameters of all interface layers

https://doi.org/10.1021/acsomega.3c08981
ACS Omega 2024, 9, 7053−7060

Table 2. Input Parameters of the Device with Different Interface Layers

properties	graphene	ZnO/Al	3C−SiC
thickness (nm)	50	50	20
band gap (eV)	1.800	3.250	2.420
electron affinity (eV)	3.92	4.000	3.830
valence band density of state ($1/cm^3$)	1.000×10^{21}	2.000×10^{18}	1.553×10^{19}
conduction band density of state ($1/cm^3$)	1.000×10^{21}	1.800×10^{19}	1.163×10^{19}
mobility of electron μ_e [$cm^2/(V\ s)$]	1.000×10^{1}	3.000×10^{2}	6.500×10^{2}
mobility of hole μ_p [$cm^2/(V\ s)$]	1.000×10^{9}	2.500×10^{1}	4.000×10^{1}
donor charge density N_D ($1/cm^3$)	0	7.250×10^{18}	1.00×10^{18}
acceptor charge density N_A ($1/cm^3$)	1.00×10^{21}	0	0
defect density N_T ($1/cm^3$)	1.00×10^{15}	1.00×10^{15}	1.00×10^{14}
references	19	20	21

are shown in Table 2. Figure 2 shows the $I-V$ and QE of the PSCs. Figure 3 shows the PSC performance with and without interface layers. Table 3 shows the comparative performance of devices with and without interface layers. When electrons and hole charge carriers are extracted and transported between the perovskite layer and the appropriate electron and HTLs, interface layers impact how well they do so. Recombination losses can be decreased with properly constructed interface layers, increasing the solar cell's efficiency.[18] Effective charge carrier extraction also depends on the energy levels of the interface layers with the absorber and charge transport layers. An effective charge transfer has facilitated energy loss at these interfaces, minimized by interface layers with the proper energy-level alignment. The enhancement of electrical conductivity, quick charge transfer, widespread solar absorption, better light trapping, and other advantageous characteristics are all made possible by including graphene in PV devices, improving their overall performance.[9] Overall, we have obtained an increase in the performance of PSCs with the addition of the graphene interface at the HTL and perovskite layer and the 3C−SiC interface layer at the ETL and perovskite layer. We have attained PCE = 27.55%, FF = 82.53%, J_{sc} = 32.63, and V_{oc} = 1.02 V.

3.2. Optimization of the Absorber Layer Thickness. The perovskite layer thickness plays a crucial role in verifying the performance of a cell. The perovskite layer thickness is a critical factor that can significantly impact the cells' performance. In a planar-type solar cell, the photon absorption efficiency is inversely related to carrier collection efficiency within the cell. The perovskite layer thickness was adjusted from 100 to 1500 nm in our structure, and the performance varied, as shown in Figure 4. When the absorber material in the solar cell is thick, it can absorb more photons due to increased interaction with incoming sunlight.[22] When the thickness of the perovskite layer is greater than the carrier diffusion length, the charge carrier formed around the middle of the layer tends to recombine before reaching the electrodes. Numerical analysis allows for the input of known material parameters and the study of the behavior of charge carriers within the perovskite layer. The diffusion length is a key metric that helps to determine how far carriers can travel without recombining. However, the contribution of photons that cross the perovskite materials' energy band gap causes a steady and quick improvement in the J_{sc} value. The photocurrent was increased even in thicker absorber devices by these higher-energy photons producing more charge carriers.[23] Conversely, when the absorber layer thickness is insignificant, the absorption of long-wavelength photons becomes limited. The thin absorber layer may not effectively absorb these lower-energy photons, resulting in lower photocurrent generation.[18]

Therefore, finding the right balance in the absorber thickness is crucial for maximizing the efficiency of PSCs. An optimal thickness ensures sufficient photon absorption across a wide range of wavelengths while minimizing carrier recombination within the absorber layer. This balance is essential to achieve high-performance solar cells.

For a thickness of 100−700 nm, J_{sc} grows swiftly from 18.39 to 34.00 mA/cm^2. Beyond that, it steadily rises until all the light is absorbed, which saturates at around 35 mA/cm^2 or 100−200 nm. J_{sc} is extremely low due to decreased absorption and utilizing thicker (>700 nm) sheets has little advantage. Considering this, a 600−700 nm perovskite layer thickness is

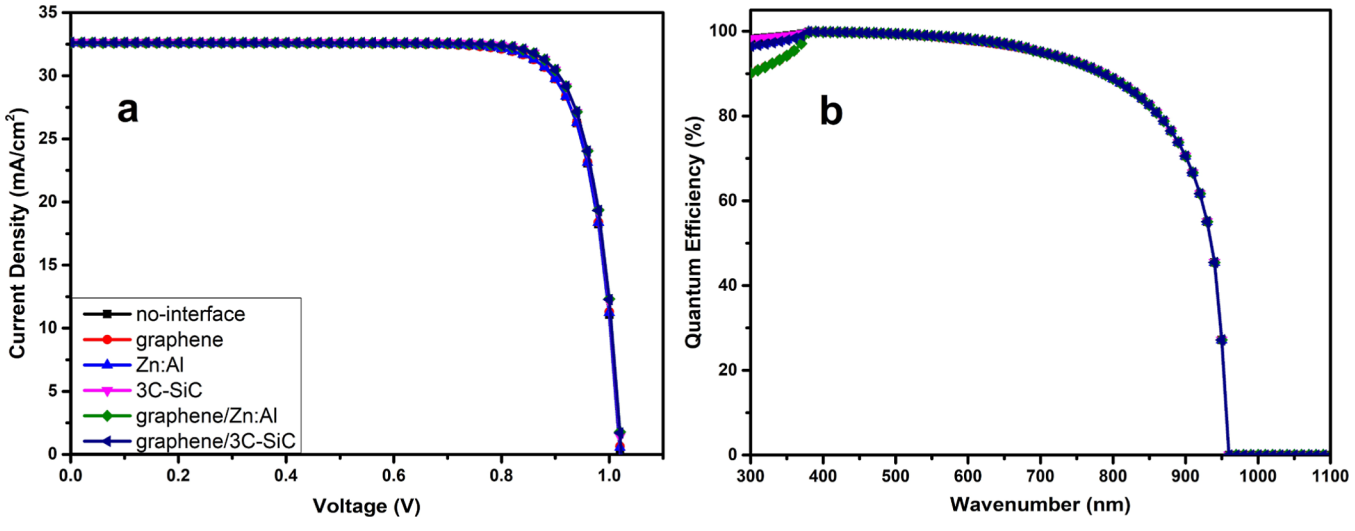

Figure 2. (a) JV and (b) QE of the PSC with and without an interface layer.

https://doi.org/10.1021/acsomega.3c08981
ACS Omega 2024, 9, 7053−7060

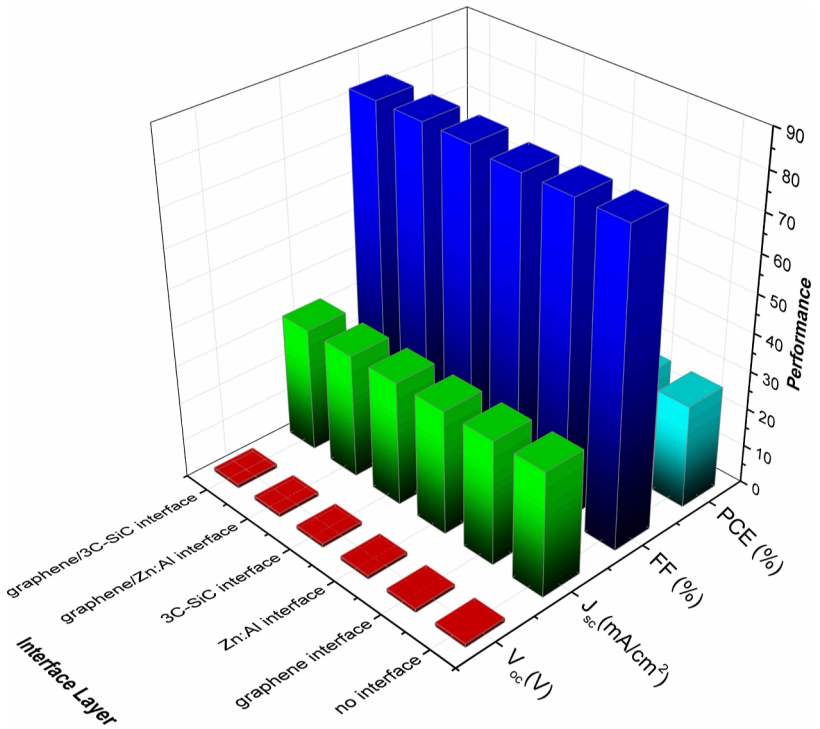

Figure 3. Performance of the $MASnBr_3$-based PSC with and without the interface layer.

Table 3. Device Performance with Different Interface Layers in the Structures

interface layers	V_{oc} (V)	J_{sc} (mA/cm^2)	FF (%)	PCE (%)
no interface	1.02	32.59	81.19	27.02
graphene	1.02	32.56	81.23	27.02
ZnO/Al	1.02	32.59	81.21	27.03
3C−SiC	1.02	32.63	82.52	27.54
graphene, ZnO/Al	1.02	32.60	82.54	27.53
graphene, 3C−SiC	1.02	32.63	82.53	27.55

appropriate. In our research, a 700 nm perovskite layer thickness was shown to have an optimized J_{sc}.

As the perovskite layer thickness increases in a device, it generates more charge carriers due to improved photon absorption. However, the collection efficiency of these carriers tends to decrease in thicker cells, primarily due to the increased likelihood of recombination. Carrier recombination occurs when the charge carriers (electrons and holes) meet and neutralize each other before they can be extracted as an electrical current at the electrodes. This reduction in carrier collection efficiency significantly impacts the V_{oc} of the device.[24]

When the perovskite layer thickness goes above the carrier diffusion length, as more carriers are generated toward the center of the absorber, they have a higher chance of recombining before reaching the electrodes. As a result, the V_{oc} of the solar cell drops with rising absorber thickness.

As the absorber layer thickness in a device increases, the fill factor tends to decrease due to rising series resistance across the device. The enhancement in series resistance occurs because, in thicker cells, the distance that charge carriers need to travel to reach the electrodes becomes longer. This increases resistance along the carrier pathways, impeding the current flow through the cell. Consequently, the series resistance negatively impacts the FF of the solar cell.

The efficiency of the cell exhibits a steady increase up to an absorber layer thickness of 700 nm, primarily driven by an increase in the J_{sc}. The solar cell efficiency is maximum at 27.97% for absorber thicknesses beyond 700 nm. This efficiency is maximum due to the maximum light absorption at this wavelength.

3.3. Optimization of Defect Density of the Perovskite Layer. The efficiency of the cell was changed by changing the defect concentration in the perovskite layer, as depicted in Figure 5. The cell parameters for different doping densities within the perovskite layer range from 10^{13} to 10^{18} cm^{-3}. As the doping level rises above 10^{13} cm^{-3}, the devices' built-in electric field (V_{bi}) also increases. This stronger V_{bi} enhances the effective separation of photogenerated carriers, leading to enhanced solar cell efficiency. An excessively high p-type level in the perovskite layer can hinder the movement of hole charge from the perovskite material to the HTL. This limitation occurs because of an elevated impurity scattering and recombination rate within the absorber, which disrupts the efficient transportation of holes.

In our case, the device J_{sc} remains relatively constant at lower doping densities. However, as the doping density increases, the J_{sc} starts to decrease gradually. This behavior was attached to recombination rates and charge carrier mobility. On the other hand, the solar cells' open-circuit voltage (V_{oc}) remains constant at lower doping densities. As the doping density increases, V_{oc} begins to increase gradually. This phenomenon is often a result of reduced trap-assisted recombination and enhanced charge carrier extraction with moderate doping levels, which enhance the fill factor with increasing doping density. The increase in doping density contributes to decreases in the sheet resistance of the perovskite layer, which allows for better charge carrier transport within the cell, leading to an improved collection efficiency and fill factor. Our numerical results show the highest efficiency of 31.94% for acceptor doping concentration at 10^{18} cm^{-3}.

https://doi.org/10.1021/acsomega.3c08981
ACS Omega 2024, 9, 7053−7060

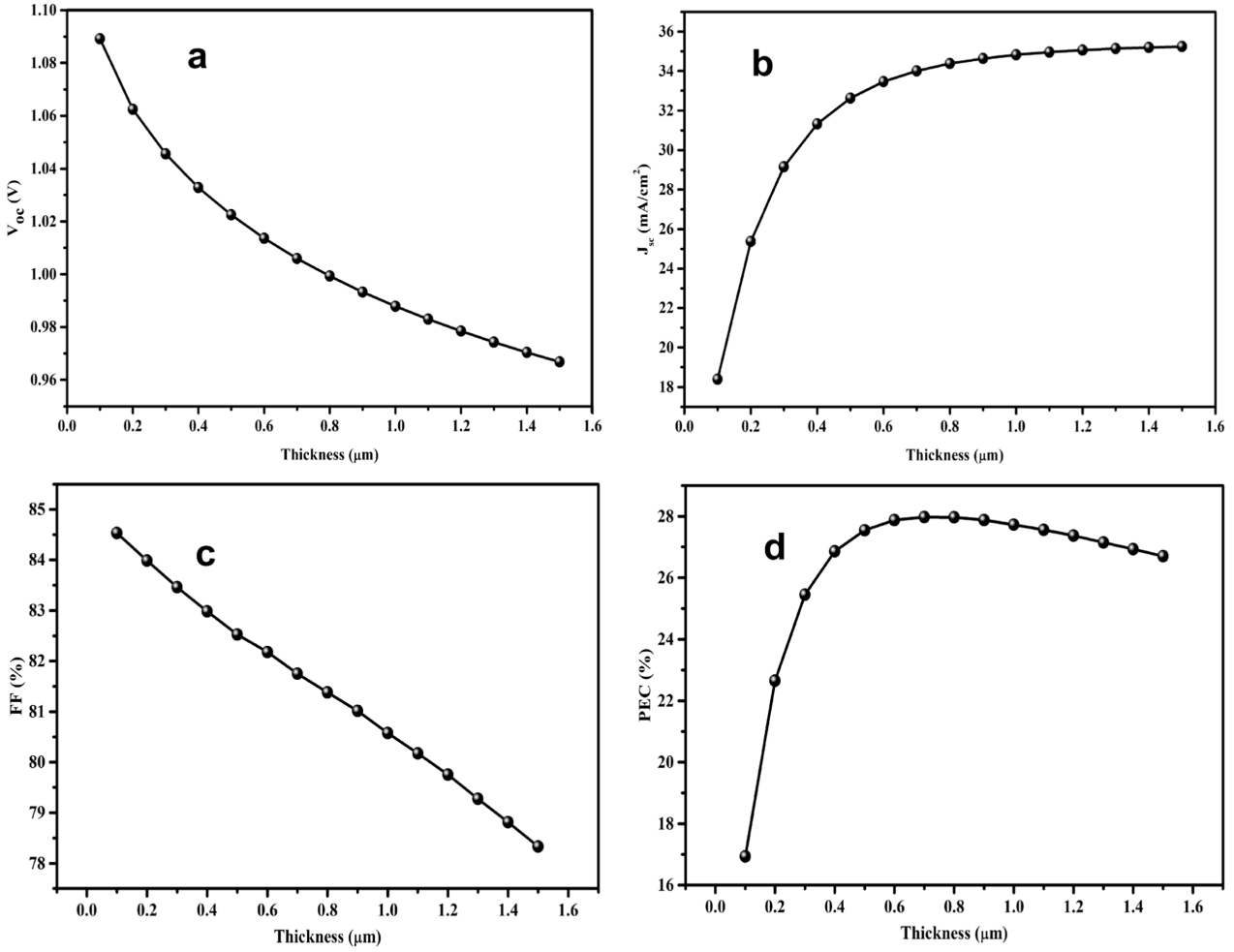

Figure 4. (a−d) Influence of the cell parameters of the PSCs with varying absorber layer thickness.

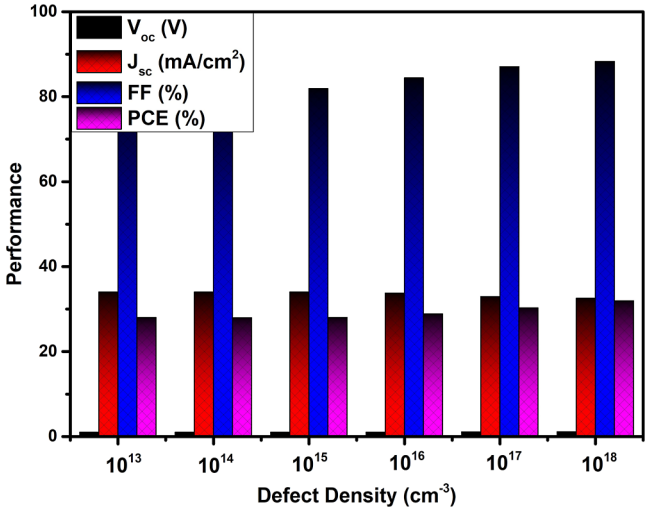

Figure 5. Perovskite layer defect concentration effect on the perovskite device.

3.4. Optimization of Graphene Thickness and Acceptor Density. The thickness of the graphene used as the interface layer between the HTL and the perovskite layer in a solar cell significantly influences its performance. In our study, we present the cell parameters for different thicknesses of the HTL interface layer within the absorber layer, varying from 0.01 to 0.3 μm, as shown in Figure 6. All the cell parameters show enhancement with increasing thickness. The HTL plays a crucial role in facilitating the transportation of positive charge carriers (holes) from the active layer to the electrode. This process is vital for optimizing the overall efficiency of the device. Our results indicate that the highest J_{sc}, V_{oc}, FF, and overall efficiency values are 32.54 mA/cm^2, 1.1197 V, 88.39%, and 31.97%, respectively, for an HTL interface layer thickness of 0.3 μm.

Figure 7 shows the impact on the PSCs' performance by changing the graphene interface's defect concentration. The efficiency of the cell can be significantly affected by the density of the acceptor sites within the HTL interface. In our case, the acceptor density of the HTL interface layer varies from 10^{13} to 10^{21} cm^{-3}. All cell parameters are enhanced by increasing the thickness. The acceptor density determines the availability of sites for positive charge carriers (holes) to move through the HTL, affecting charge transport and recombination dynamics. Our results show optimized cell parameters at 10^{21} cm^{-3}.

3.5. Optimization of 3C−SiC Thickness and Donor Density. The perovskite of the proposed cell was evaluated by changing the thickness of the 3C−SiC interface layer between the ETL and the absorber layer. Our study explored a range of interface layer thicknesses from 0.005 to 0.1 μm, as shown in Figure 8. The maximum performance, 31.97%, was achieved at a thickness of 0.015 μm. The impact of these different thicknesses on crucial performance metrics, such as V_{oc}, J_{sc}, FF, and conversion efficiency, is illustrated in the accompanying figure.

https://doi.org/10.1021/acsomega.3c08981
ACS Omega 2024, 9, 7053−7060

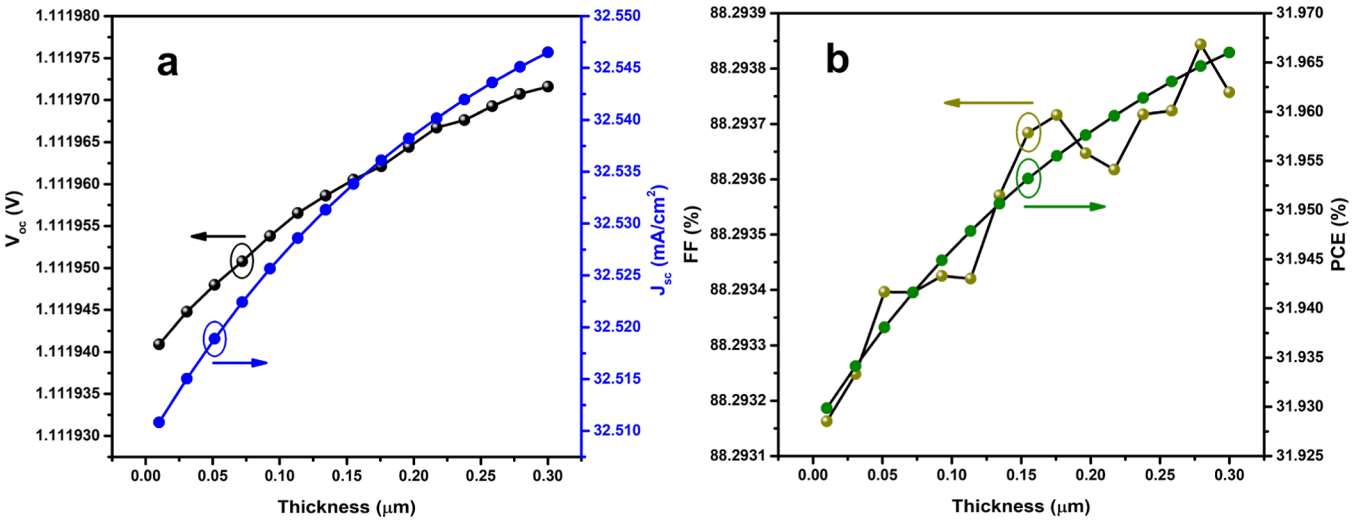

Figure 6. (a,b) Impact on the efficiency of PSCs by changing the thickness of graphene used as the interface layer.

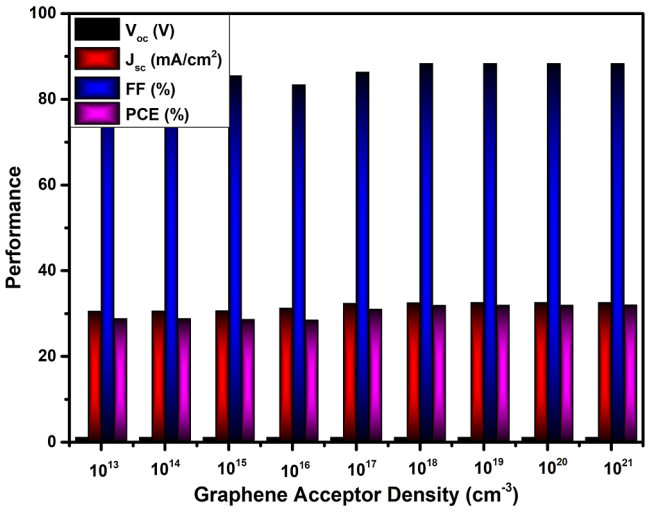

Figure 7. Effect of graphene charge density on the performance of the $MASnBr_3$-based PSC.

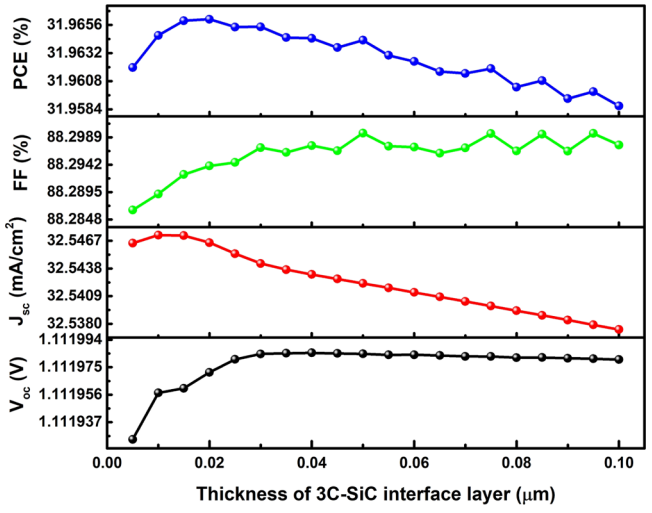

Figure 8. Impact on the efficiency of PSCs by changing the thickness of 3C−SiC used as the interface layer.

To investigate the effect of the donor density within the ETL interface layer on the cell efficiency, we varied the donor concentration in the range of 10^{13} to 10^{21} cm^{-3}, as shown in Figure 9. Figure 9 shows the performance metrics, including V_{oc},

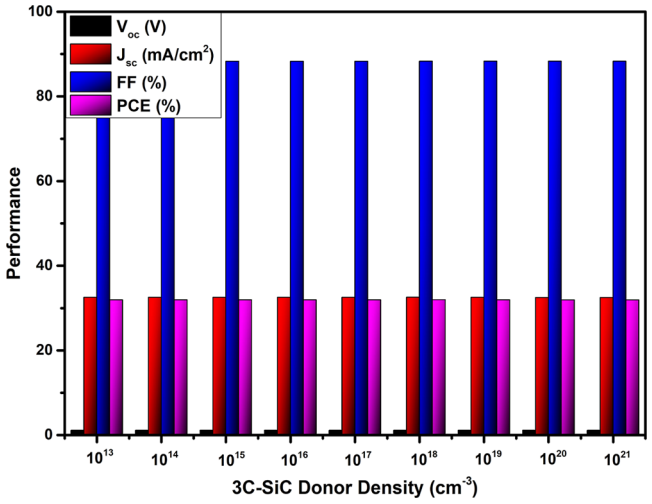

Figure 9. Influence of the 3C−SiC donor density on the performance of the $MASnBr_3$-based PSC.

J_{sc}, FF, and PCE, for the ETL interface layer donor density. The results indicate that both V_{oc} and J_{sc} exhibit a relatively consistent trend as the donor density within the ETL interface layer increases. In contrast, conversion efficiency values remain relatively constant beyond the threshold of 10^{17} cm^{-3}. Furthermore, it is noteworthy that the conversion efficiency reaches its maximum when the donor densities exceed 10^{18} cm^{-3} and then gradually decrease.

3.6. Optimized Performance. The optimized perovskite device structure with an interface layer is illustrated in Figure 10. Figure 10 shows the QE wavelength and the $I-V$ curve, demonstrating the enhanced performance of the PSC. The optimal PSC efficiency metrics are as follows: PCE = 31.97%, V_{oc} = 1.112 V, J_{sc} = 32.54 mA/cm^2, and FF = 89.38%. The optimized performance is much higher than the conventional silicon solar cell and recent developments in PSCs.[25−28]

https://doi.org/10.1021/acsomega.3c08981
ACS Omega 2024, 9, 7053−7060

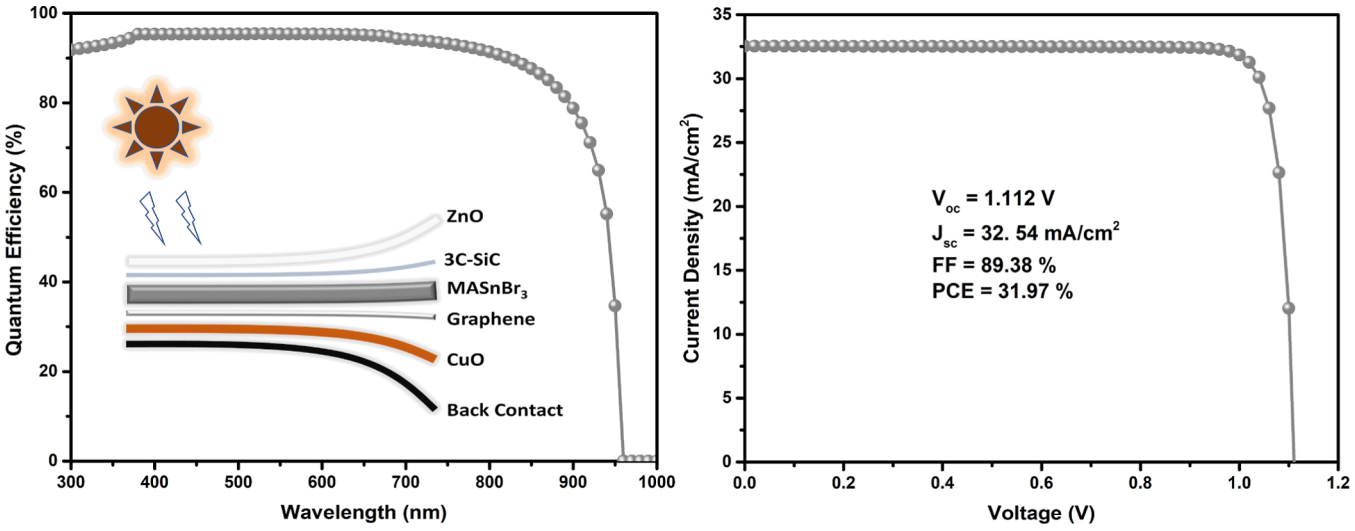

Figure 10. *I*−*V* and QE of the final structure of the optimized structure with different interface layers.

4. CONCLUSIONS

In summary, this research systematically improved the efficiency of lead-free $MASnBr_3$ solar cells by implementing interface layers in the structures using SCAPS-1D numerical software. We used the interface layer of graphene between the HTL and the absorber layer and ZnO/Al and 3C−SiC interface layers between the ETL and the perovskite layer. The study systematically examined variations in layer thickness of the absorber layer, graphene layer, and 3C−SiC, doping density of all layers, and interface density of active materials. Furthermore, the recombination and generation rate, *I*−*V*, and QE were determined to explore the solar cell properties and prospects. We adjusted the thicknesses and defect densities of the absorber layer and interface layers. The optimized structure ZnO/3C−SiC/$MASnBr_3$/graphene/CuO/Au obtained the maximum performance with the best quantum efficiency of 94%. We obtained the PCE = 31.97%, FF = 89.38%, J_{sc} = 32.54 mA/cm^2, and V_{oc} = 1.112 V. These results enhance our comprehension of lead-free PSCs and open the path for the development and production of more environmentally friendly, high-efficiency solar cells.

AUTHOR INFORMATION

Corresponding Authors

Sofia Tahir − *Department of Physics, Government College University Faisalabad, 38000 Faisalabad, Punjab, Pakistan*; Email: sofetahir@gmail.com

Arslan Ashfaq − *Department of Physics, Government College University Faisalabad, 38000 Faisalabad, Punjab, Pakistan*; orcid.org/0000-0003-0958-2396; Email: arslan.ashfaq201@gmail.com

Authors

Muhammad Haneef − *Department of Physics, Government College University Faisalabad, 38000 Faisalabad, Punjab, Pakistan*

Haitham A. Mahmoud − *Department of Industrial Engineering, College of Engineering, King Saud University, Riyadh 11421, Saudi Arabia*

Adnan Ali − *Department of Physics, Government College University Faisalabad, 38000 Faisalabad, Punjab, Pakistan; London Centre for Energy Engineering (LCEE), School of Engineering, London South Bank University, London SE1 0AA, U.K.*

Complete contact information is available at: https://pubs.acs.org/10.1021/acsomega.3c08981

Author Contributions

Muhammad Haneef: Software; **Sofia Tahir:** Writing—Review & Editing, Supervisor; **Haitham A. Mahmoud:** Formal Analysis; **Adnan Ali:** Visualization; **Arslan Ashfaq:** Writing—Original Draft, Conceptualization.

Notes

The authors declare no competing financial interest.

ACKNOWLEDGMENTS

The authors would like to acknowledge the British Council for their funding under PAK-UK ICRG 2020 project (006327/D/ISB/008/2021) to create a research group of students and establishment of "Semiconductor Physics and Renewable Energy Laboratory" (SPREL) at Government College University Faisalabad Pakistan. The authors present their appreciation to King Saud University for funding this research through Researchers Supporting Program number (RSPD2023R1006), King Saud University, Riyadh, Saudi Arabia.

REFERENCES

(1) Sharma, R.; Sharma, A.; Agarwal, S.; Dhaka, M. Stability and efficiency issues, solutions and advancements in perovskite solar cells: a review. *Sol. Energy* **2022**, *244*, 516−535.

(2) Najim, A.; Bajjou, O.; Bakour, A.; Boulghallat, M.; Rahmani, K. A fundamental study on the electronic and optical properties of graphene oxide under an external electric field. *Mod. Phys. Lett. B* **2023**, *38*, 2450032.

(3) Shamna, M.; Nithya, K.; Sudheer, K. Simulation and optimization of $CH_3NH_3SnI_3$ based inverted perovskite solar cell with NiO as Hole transport material. *Mater. Today: Proc.* **2020**, *33*, 1246−1251.

(4) Moulaoui, L.; Bajjou, O.; Najim, A.; Rahmani, K.; Marouane, A.; Laassouli, A.; Lachtioui, Y.; Manaut, B. Numerical Simulation of $FAPbI_3$ perovskite based solar cells with graphene oxide as hole transport layer using SCAPS-1D. In *2023 3rd International Conference on Innovative Research in Applied Science; Engineering and Technology (IRASET)*; IEEE, 2023; pp 1−7.

(5) Shenoy, U. S.; Goutham, K. D.; Bhat, D. K. A case of perfect convergence of light and heavy hole valence bands in SnTe: the role of Ge and Zn co-dopants. *Mater. Adv.* **2022**, *3*, 5941−5946.
(6) Chandrasekhar, P.; Dubey, A.; Qiao, Q. High efficiency perovskite solar cells using nitrogen-doped graphene/ZnO nanorod composite as an electron transport layer. *Sol. Energy* **2020**, *197*, 78−83.
(7) Jamil, M.; Almufarij, R. S.; Ali, A.; Ashfaq, A.; Mahmood, K.; Fahmy, M. A.; Sabugaa, M. M.; Alqurashi, R. S.; Shokralla, E. A.; Algethami, O. A. Improving the Recombination Losses by the Inclusion of Bi-HTM (CuO/Silicon) Layers for Formamidinium Tin-Based Perovskite Solar Cells. *Adv. Theory Simul.* **2023**, *6*, 2300106.
(8) Slami, A.; Bouchaour, M.; Merad, L. Comparative study of modelling of Perovskite solar cell with different HTM layers. *Int. J. Mater.* **2020**, *7*, 1.
(9) Mohseni, H.; Dehghanipour, M.; Dehghan, N.; Tamaddon, F.; Ahmadi, M.; Sabet, M.; Behjat, A. Enhancement of the photovoltaic performance and the stability of perovskite solar cells via the modification of electron transport layers with reduced graphene oxide/polyaniline composite. *Sol. Energy* **2021**, *213*, 59−66.
(10) Ehrmann, N.; Reineke-Koch, R. Ellipsometric studies on ZnO: Al thin films: Refinement of dispersion theories. *Thin Solid Films* **2010**, *519*, 1475−1485.
(11) Sameera, J. N.; Islam, M. A.; Islam, S.; Hossain, T.; Sobayel, M.; Akhtaruzzaman, M.; Amin, N.; Rashid, M. J. Cubic Silicon Carbide (3C−SiC) as a buffer layer for high efficiency and highly stable CdTe solar cell. *Opt. Mater.* **2022**, *123*, 111911.
(12) Devi, C.; Mehra, R. Device simulation of lead-free $MASnI_3$ solar cell with $CuSbS_2$ (copper antimony sulfide). *J. Mater. Sci.* **2019**, *54*, 5615−5624.
(13) Mushtaq, S.; Tahir, S.; Ashfaq, A.; Sebastian Bonilla, R.; Haneef, M.; Saeed, R.; Ahmad, W.; Amin, N. Performance optimization of lead-free $MASnBr_3$ based perovskite solar cells by SCAPS-1D device simulation. *Sol. Energy* **2023**, *249*, 401−413.
(14) Shivesh, K.; Alam, I.; Kushwaha, A. K.; Kumar, M.; Singh, S. V. Investigating the theoretical performance of Cs_2TiBr_6-based perovskite solar cell with La-doped $BaSnO_3$ and $CuSbS_2$ as the charge transport layers. *Int. J. Energy Res.* **2022**, *46*, 6045−6064.
(15) Moulaoui, L.; Bajjou, O.; Lachtioui, Y.; Najim, A.; Archi, M.; Rahmani, K.; Manaut, B. Modeling of Highly Efficient Lead-Free $MASnI_3$-Based Solar Cell with Graphene Oxide as Hole Transport Layer Using SCAPS-1D. *J. Electron. Mater.* **2023**, *52*, 7541−7553.
(16) ur Rehman, U.; Almousa, N.; ul Sahar, K.; Ashfaq, A.; Mahmood, K.; Shokralla, E. A.; Al-Buriahi, M. S.; Alrowaili, Z. A.; Capangpangan, R. Y.; Alguno, A. C. Optimizing the Efficiency of Lead-Free Cs_2TiI_6-Based Double Halide Perovskite Solar Cells Using SCAPS-1D. *Energy Technol.* **2023**, *11*, 2300459.
(17) Zhang, X.; Zhou, H.; Hu, C.; Zhao, Y.; Ma, X.; Wu, J.; Qi, Y.; Fang, W.; Jia, S.; Yu, J. Performance analysis of all-inorganic $Cs_3Sb_2I_9$ perovskite solar cells with micro-offset energy level structure by SCAPS-1D simulation and First-principles calculation. *Sol. Energy Mater. Sol. Cells* **2023**, *260*, 112487.
(18) Almufarij, R. S.; Ashfaq, A.; Tahir, S.; Alqurashi, R. S.; Ragab, A. H.; El-Refaey, D.; Mushtaq, S.; Shokralla, E. A.; Ali, A.; Capangpangan, R. Y.; et al. Improving performance and recombination losses in lead free formamidinium tin based perovskite solar cells. *Mater. Chem. Phys.* **2023**, *307*, 128150.
(19) Danladi, E.; Egbugha, A. C.; Obasi, R. C.; Tasie, N. N.; Achem, C. U.; Haruna, I. S.; Ezeh, L. O. Defect and doping concentration study with series and shunt resistance influence on graphene modified perovskite solar cell: a numerical investigation in SCAPS-1D framework. *J. Indian Chem. Soc.* **2023**, *100*, 101001.
(20) Alias, N. S. N. M.; Arith, F.; Mustafa, A.; Ismail, M.; Chachuli, S.; Shah, A. Compatibility of Al-doped ZnO electron transport layer with various HTLs and absorbers in perovskite solar cells. *Appl. Opt.* **2022**, *61*, 4535−4542.
(21) Agha, D. N. Q.; Algwari, Q. T. The influence of the interface layer between the electron transport layer and absorber on the performance of perovskite solar cells. *IOP Conference Series: Materials Science and Engineering*; IOP Publishing, 2021.
(22) Tahir, S.; Ashfaq, A.; Mushtaq, S.; Haneef, M.; Saleh Alqurashi, R.; Ali Shokralla, E.; Sabugaa, M. M.; Almufarij, R. S.; Rehman, U. . u.; Bonilla, R. S. Performance optimization of inorganic Cs_2TiBr_6 based perovskite solar cell via numerical simulation. *Energy Technol.* **2023**, *11*, 2300359.
(23) Ashfaq, A.; Tahir, S.; Mushtaq, S.; Alqurashi, R. S.; Haneef, M.; Almousa, N.; Rehman, U. u.; Bonilla, R. S. Comparative performance analysis of Cs_2TiX_6 (X= Br-Cl-I-) lead-free perovskite solar cells incorporating single, double and triple layer halides by SCAPS− 1D. *Mater. Today Commun.* **2023**, *35*, 106016.
(24) Najim, A.; Bajjou, O.; Bakour, A.; Moulaoui, L.; Rahmani, K. Numerical computing of CdTe-based solar cells with graphene oxide buffer layers using SCAPS-1D software. *Indian J. Phys.* **2023**, *98*, 67−77.
(25) Yang, W. S.; Noh, J. H.; Jeon, N. J.; Kim, Y. C.; Ryu, S.; Seo, J.; Seok, S. I. J. S. High-performance photovoltaic perovskite layers fabricated through intramolecular exchange. *Science* **2015**, *348*, 1234−1237.
(26) Yang, W. S.; Park, B.-W.; Jung, E. H.; Jeon, N. J.; Kim, Y. C.; Lee, D. U.; Shin, S. S.; Seo, J.; Kim, E. K.; Noh, J. H.; et al. Iodide management in formamidinium-lead-halide−based perovskite layers for efficient solar cells. *Science* **2017**, *356*, 1376−1379.
(27) Zhou, X.; Zhang, L.; Wang, X.; Liu, C.; Chen, S.; Zhang, M.; Li, X.; Yi, W.; Xu, B. Highly efficient and stable GABr-modified ideal-bandgap (1.35 eV) Sn/Pb perovskite solar cells achieve 20.63% efficiency with a record small Voc deficit of 0.33 V. *Adv. Mater.* **2020**, *32*, 1908107.
(28) Tahir, S.; Saeed, R.; Ashfaq, A.; Ali, A.; Mehmood, K.; Almousa, N.; Shokralla, E. A.; Macadangdang, R. R., Jr.; Soeriyadi, A. H.; Bonilla, R. S. Optical modeling and characterization of bifacial SiNx/AlOx dielectric layers for surface passivation and antireflection in PERC. *Prog. Photovoltaics Res. Appl.* **2023**, *32*, 63−72.

https://doi.org/10.1021/acsomega.3c08981
ACS Omega 2024, 9, 7053−7060